J Appl Biomater Function Mater 2012; Vol. 10 no. 2, 119-126
DOI: 10.5301/JABFM.2012.9706

ORIGINAL ARTICLE

Preparation and characterization of shape memory polymer scaffolds via solvent casting/particulate leaching

Luigi De Nardo[1], Serena Bertoldi[2], Alberto Cigada[1], Maria Cristina Tanzi[2], Håvard Jostein Haugen[3], Silvia Farè[2]

[1]Department of Chemistry, Materials, and Chemical Engineering "G. Natta", Politecnico di Milano, Milano - Italy
[2]Biomaterials Laboratory, Department of Bioengineering, Politecnico di Milano, Milano - Italy
[3]Biomaterials Department, Institute for Clinical Dentistry, University of Oslo, Oslo - Norway

ABSTRACT

Purpose: **Porous Shape Memory Polymers (SMPs) are ideal candidates for the fabrication of defect fillers, able to support tissue regeneration via minimally invasive approaches. In this regard, control of pore size, shape and interconnection is required to achieve adequate nutrient transport and cell ingrowth. Here, we assessed the feasibility of the preparation of SMP porous structures and characterized their chemico-physical properties and in vitro cell response.**

Methods: **SMP scaffolds were obtained via solvent casting/particulate leaching of gelatin microspheres, prepared via oil/water emulsion. A solution of commercial polyether-urethane (MM-4520, Mitsubishi Heavy Industries) was cast on compacted microspheres and leached-off after polymer solvent evaporation. The obtained structures were characterized in terms of morphology (SEM and micro-CT), thermo-mechanical properties (DMTA), shape recovery behavior in compression mode, and in vitro cytocompatibility (MG63 Osteoblast-like cell line).**

Results: **The fabrication process enabled easy control of scaffold morphology, pore size, and pore shape by varying the gelatin microsphere morphology. Homogeneous spherical and interconnected pores have been achieved together with the preservation of shape memory ability, with recovery rate up to 90%. Regardless of pore dimensions, MG63 cells were observed adhering and spreading onto the inner surface of the scaffolds obtained for up to seven days of static in vitro tests.**

Conclusions: **A new class of SMP porous structures has been obtained and tested in vitro: according to these preliminary results reported, SMP scaffolds can be further exploited in the design of a new class of implantable devices.**

Key words: Cytocompatibility, In vitro Studies, Porous Materials, Shape Memory Polymers, Smart materials

Accepted: December 29, 2011

INTRODUCTION

Minimally invasive surgery (MIS) emerged as a powerful clinical option that enables implantation procedures through natural body openings or small artificial incisions; this approach significantly improved the healthcare system, both in terms of the patients quality life and medical costs. By affecting the techniques used in every specialty of surgical medicine (1), MIS not only led to new therapeutic opportunities, but opened up new challenging problems in the selection or synthesis of biomaterials, that have to show suitable functional properties (2-4).

Thermally activated Shape Memory Polymers (SMP) hold a high potential in this context (5-7): they possess the ability to memorize a permanent shape, that can significantly differ from their temporary one, and can be locally recovered by applying a temperature increase above the switching transition temperature (T_{trans}) (8-10). A thermally induced shape memory effect has been reported for different classes of materials (7): shape memory alloys (SMAs), mainly nickel-titanium alloys, have already been extensively used in clinical practice to meet some MIS requirements (5-7). In the last 20 years, several polymeric systems with shape memory ability have been synthesized (11-14), and their potential uses proposed by several research groups (4,8,9,11,15,16).

When compared to SMAs, SMPs show the ability to recover larger deformations (up to 800%), biocompatibility (17), lower costs, and simpler processing (3). The latter aspect is of particular importance for two main reasons. Physical and mechanical properties of SMPs can be adjusted by slight variations in their chemical composition and structure (3,11,18): it is thus possible to tailor specific combinations of SMP properties required for specific applications (*e.g.* T_{trans}) (4,19). Moreover, easy processing enables to obtain complex structures, such as cellular solids, without impairing the shape memory ability (20). The possibility of controlling porous structures, in terms of pore

dimension and interconnection, is straightforward in the design of materials for fillers promoting integration in the host tissue. For instance, fillers for the repair of injured tissues can be manufactured by using SMP (21,22), exploiting the ability of in situ recovery of a large predetermined permanent shape (10,11).

Here, we assessed the feasibility of obtaining SMP porous scaffolds via solvent casting/particulate leaching and assessed their in vitro biocompatibility. The cellular solids obtained have been optimized to exhibit different morphologies and mechanical properties, without affecting thermal and shape memory properties.

MATERIALS AND METHODS

Sample preparation

Porous scaffolds were obtained from a commercial aromatic poly(ether urethane) with shape memory properties (MM-4520, Mitsubishi H.I. Ltd., Japan), by using the solvent casting/particulate leaching technique, as previously reported (20,23). In short, gelatine was dissolved in water at high concentration and the solution was added to a beaker containing soybean oil, heated to 60°C under continuous stirring. After a few minutes, the emulsion was cooled down to 15°C in an ice bath, and gelatine droplets were dehydrated by adding cold acetone. Gelatine microspheres were removed from soybean oil, washed several times with acetone and then dried. Microspheres were sieved to obtain two different ranges of dimensions: Ø<150 μm (scaffold with smaller porosity, SP) and 150 μm<Ø<400 μm (scaffold with larger porosity, LP). The microspheres obtained were leveled in a glass mould to a 3 mm thickness and placed in an oven for up to 96 hours with 95% relative humidity at T = 50°C, in order to achieve adhesion of the gelatine microspheres. MM-4520 was dissolved in chloroform (3% w/v solution) and cast onto compacted gelatine microspheres. After vacuum drying, 5 mm diameter samples were punched out from the sheets before dissolving the porogen by washing the scaffolds several times with deionized water. All samples were dried in air and kept in a desiccator until characterization.

MATERIAL CHARACTERIZATION

Scaffold morphology

The morphology of the obtained porous structures, both along the surface and the cross-section, was assessed by Scanning Electron Microscopy (SEM). Samples were gold sputter-coated (Edwards S150B, operating at 0.2 mbar, 1 kV, 20 mA for 1 min) and observed with a StereoScan 360 SEM (Cambridge) at 10 kV.

Morphologic characterization by micro-CT

Porosity, average pore size, pore size distribution, and pore interconnection were assessed by micro-CT analysis. The scaffolds were analyzed using a 1172 micro-CT imaging system (Skyscan, Aartselaar, Belgium) at 5 μm voxel resolution, X-ray tube current 173 μA, and voltage 60 kV without any filters. The specimens were rotated through 180° around the long axis of the sample, with a rotation of 0.4°. The projection radiographs of the scaffold were reconstructed to serial coronal-oriented tomograms using a 3D cone beam reconstruction algorithm, setting the beam hardening to 20% and the ring artifact reduction to 12. Tridimensional reconstruction of the internal pore morphology was performed using axial bitmap images and analyzed by CTan and CTvol software (Skyscan, Aartselaar, Belgium). The grey scale threshold was set between 45 and 255, removing all objects smaller than 300 voxels and not connected to the 3D model (despeckling function). In order to eliminate potential edge effects, the cylindrical volume of interest (VOI) was selected in the center of a scaffold (Ø=2.5 mm, h=2 mm). Scaffold porosity was then calculated according to the following equation [1]:

$$\text{Porosity (\%)} = 100\ (1 - V_B) \qquad \text{[Eq. 1]}$$

where V_B is the binarized object volume (material sample) in VOI.

All images underwent a 3D analysis, followed by a shrink-wrap function, which enabled measuring the fraction of the pore volume accessible from the outside through openings of a certain minimum size (24). The shrink-wrap process was performed between two 3D measurements to shrink the outside boundary of the VOI in a sample through any opening whose size is equal to or larger than a threshold value (the range 0–200 μm was used in this study). Interconnectivity was then calculated according to the following equation [2]:

$$\text{Interconnectivity} = 100\ (V - V_{shrink\text{-}wrap})\ (V - V_m)^{-1} \qquad \text{[Eq. 2]}$$

where V is the total volume of the VOI, $V_{shrink\text{-}wrap}$ is the VOI volume after shrink-wrap processing, and V_m is the volume of the material. The interconnectivity pore size is hereby called cut-off pore diameter. The mean pore diameter distribution was found by measuring the material thickness on the inverse model, which was generated by setting grey scale threshold between 0 and 45.

Thermo-mechanical characterization

Dynamic Mechanical Analysis (DMA) was performed using a DMA 2980 analyzer (TA Instrument) in compression mode in the temperature range 0-180°C, with a heating rate of 1 K min^{-1}, 1 Hz and 50 μm strain application.

Storage modulus (E'), loss modulus (E'') and Tan delta (Tan δ = E''/E') were recorded. Tests were performed in duplicate, according to the ASTM 1640-99 (Standard Test Method for Assignment of the Glass Transition Temperature By Dynamic Mechanical Analysis), using cylinder specimens (Ø=5 mm, h=3 mm).

Shape memory recovery characterization

Shape memory recovery tests were performed in compression mode (DMA 2980, TA Instrument) using cylinder specimens (Ø=5 mm, h=3 mm, n=2). Each sample was heated up to a temperature $T_H=T_g+30°C$ and then compressed to $\varepsilon_m=50\%$. While maintaining the strain constant (ε_m), the sample was cooled down to $T_L=T_g-30°C$ to fix the temporary shape. At $T=T_L$, the stress was released and the sample was initially allowed to recover to ε_u and subsequently heated at a constant rate ($H_r=1$ K min^{-1}).

Values of recovered deformation as a function of temperature were recorded. Shape memory properties of the scaffolds were quantified by calculating the strain recovery rate (R_r) and recovery behavior as a function of temperature ($R_r(T)$), according to the following equation [3]:

$$R_r(T) = \frac{\varepsilon_m - \varepsilon(T)}{\varepsilon_m} \qquad \text{[Eq. 3]}$$

In vitro cytocompatibility tests

Samples were tested after sterilization in ethanol 70% (v/v in water) followed by UV irradiation (λ=254 nm) for 10 min. In vitro cytocompatibility of MM-4520 porous structures was assessed using the human osteosarcoma cell line MG63 (ECACC No. 86051601). MG63 cells were suspended in Eagle's Minimum Essential Medium (EMEM) containing: 10% fetal bovine serum (FBS) (Sigma-Aldrich), 1% non-essential amino acids (Sigma-Aldrich), 2mM L-glutamine (Sigma-Aldrich), 100 units/mL penicillin (Sigma-Aldrich), 0.100 mg/mL streptomycin (Sigma-Aldrich). The cell suspension (density = 3.0 x 10^4 cell ml^{-1}, 100 µL/well) was seeded onto each SP and LP MM-4520 specimen, placed in a 96-multiwell tissue culture plate (TCPS) and cultured in an incubator (5% CO_2, 37°C) up to seven days. TCPS (n=3) was used as positive control. Cell viability (n=3 for each sample and time point) was assessed by MTT-biochemical assay (3-(4,5-Dimethylthiazol-2-yl)-2,5-diphenyltetrazolium bromide, a tetrazole). At different time-points, culture medium was replaced with 200 µL of MTT (Sigma-Aldrich) solution and incubated for four hours at 37°C and 5% CO_2. Afterwards, MTT solution was replaced with 200µL of DMSO (Merk) and the multiwell plate was shaken until complete salt crystal dissolution. Absorbance was measured using a Tecan Genius Plus plate reader. To assess cell morphology, at each time point (3 h, 1, 3 and 7 days after seeding), SP and LP MM-4520 porous specimens (n=2 for each time-point) were fixed with 1.5% v/v glutaraldehyde solution buffered in 0.1 M sodium cacodylate (pH 7.2), dehydrated through a series of ethyl alcohol solutions (20% to 100% v/v ethyl alcohol in distilled water) and then air dried. Specimens were gold-sputtered and examined by SEM at an accelerating voltage of 7.5 kV.

RESULTS

Morphologic characterization

Figure 1 reports the SEM micrographs of the gelatin microsphere preparation after adhesion in molds at controlled temperature, humidity, and time (Fig. 1A and C). The morphology of SMP-based scaffolds prepared via solvent casting of MM-4520 polyurethane and subsequent particulate leaching, is shown in Figure 1B and D, respectively for SP and LP specimens. At SEM observation, regular spherical pores are evident, whose dimension is correlated to the starting microspheres: diameters appear to be lower than 150 µm for SP MM-4520 (Fig. 1B) and in the range 150-400 µm for SP MM-4520 (Fig. 1D). Moreover, pores are regularly distributed, showing a spherical morphology, and appear highly interconnected, with a predominance of voids. Density (calculated by weights) resulted in 0.10 g cm^{-3} for both SP and LP specimens, *vs.* 0.95 g cm^{-3} of the bulk material (20).

Results of the morphology characterization of MM-4520 SP and LP by micro-CT are reported in Table I. Open porosity values (up to 90%) were measured for both MM-4520 SP and LP. MM-4520 SP shows average pore size lower than LP scaffolds, as in SEM observation. These results are confirmed by the pore size distribution trend (Fig. 2A). MM-4520 SP scaffolds present a peak in pores size distribution at about 100 µm, while a broad peak in the range 100-200 µm can be observed for MM-4520 LP.

Quantitative assessment of pore dimension distribution and interconnection, in terms of accessible void volume at different connection size (cut-off pore diameter), was also performed by micro-CT analysis. In Figure 2B trends of accessible void volume as a function of the cut-

TABLE I - MORPHOLOGY PROPERTIES OF MM-4520 SP AND LP POROUS STRUCTURES OBTAINED VIA MICRO-CT ANALYSIS

Material	Open porosity [%]	Average pore size [µm]
MM-4520 SP	90 ± 2	116 ± 14
MM-4520 LP	91 ± 2	194 ± 26

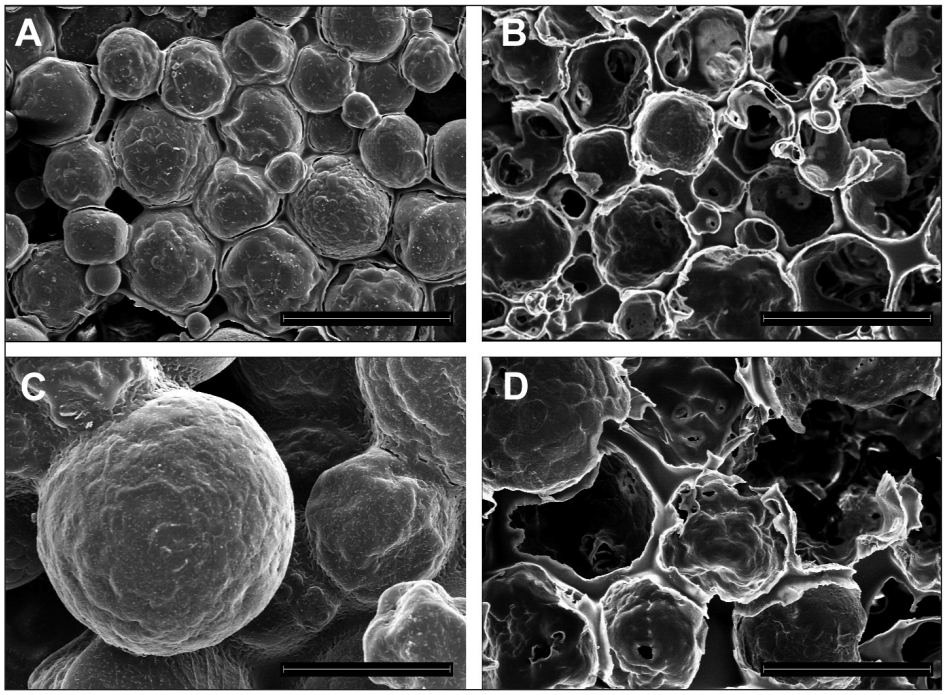

Fig. 1 - *SEM micrographs of MM-4520 scaffolds obtained via solvent casting/particulate leaching. MM-4520 SP (gelatine spheres Ø < 150 µm): (A) before and (B) after microsphere leaching in water. MM-4520 LP (gelatine spheres Ø = 150 ÷ 400 µm): (C) before and (D) after microsphere leaching in water. (Scale bar 200 µm.)*

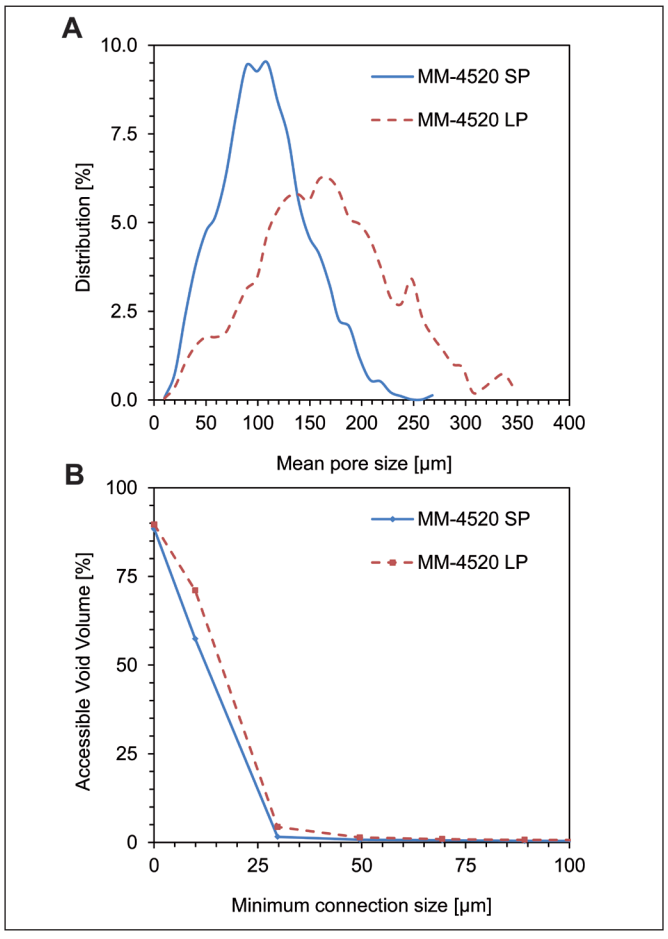

Fig. 2 - *Micro-CT analysis on MM-4520 SP and MM-4520 LP scaffolds: Trends of (A) Pores size distribution and (B) Accessible void volume at different minimum connection size.*

off pore diameter for MM-4520 SP and MM-4520 LP are reported.

Accessible void volume decreases by increasing cut-off pore diameter, thus indicating that pore interconnection decreases for higher connection size. The accessible void volume follows the same trend for both MM-4520 SP and MM-4520 LP, even if higher values of accessible void volume were observed in LP specimens at all the cut-off pore diameters up to 30 µm (at this dimension, accessible void volume drops to 0 for both structures).

Thermo-mechanical characterization

Results of DMA analysis on MM-4520 SP and LP scaffolds are reported in Figure 3A and 3B, respectively. DMA plots show a similar behavior for both specimens, whose Storage Moduli (E') resulted in 1-10 MPa range (at T=25°C) and underwent a drastic drop of nearly two orders of magnitude by increasing temperature. T_{trans} (that for this polymer system is a glass transition temperature T_g) resulted in the (48-51) °C range, as calculated from tan peak. Figure 3A and 3B also show the behavior of recovery rate as a function of temperature: a typical sigmoidal recovery curve was obtained, scaffolds with larger porosity (LP) being characterized by a higher final R_r.

In vitro cytocompatibility tests

Results of the proliferation experiments at different time points (up to seven days of culture) are summarized in Figure 4. It is possible to notice an increase in cell proliferation with time for both porous structures.

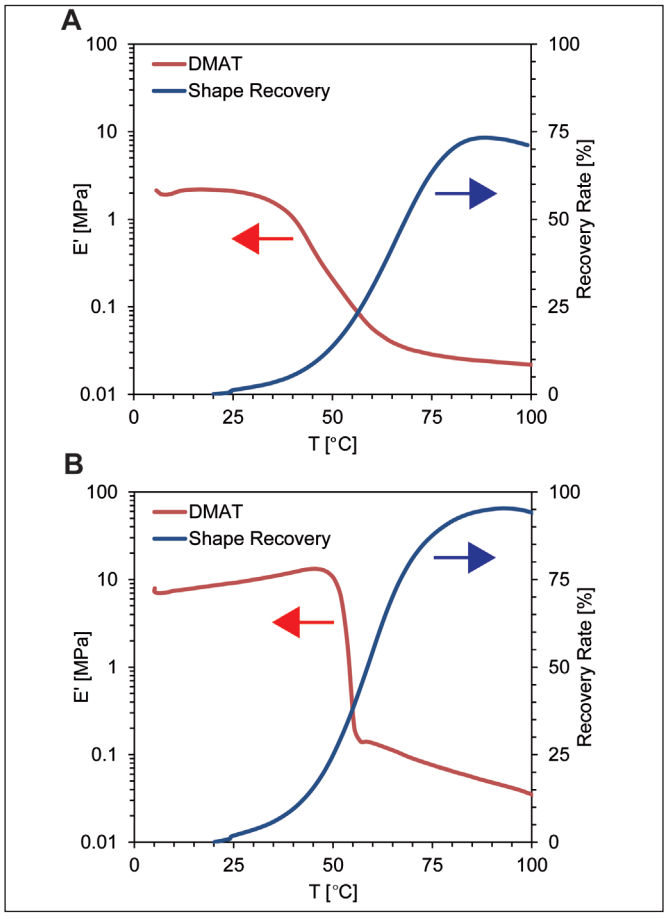

Fig. 3 - *Thermo-mechanical (storage modulus) and shape recovery (recovery rate) tests for MM-4520 scaffolds with (A) small (SP, Ø < 150 µm) and (B) large (LP, Ø = 150 ÷ 400 µm) porosity.*

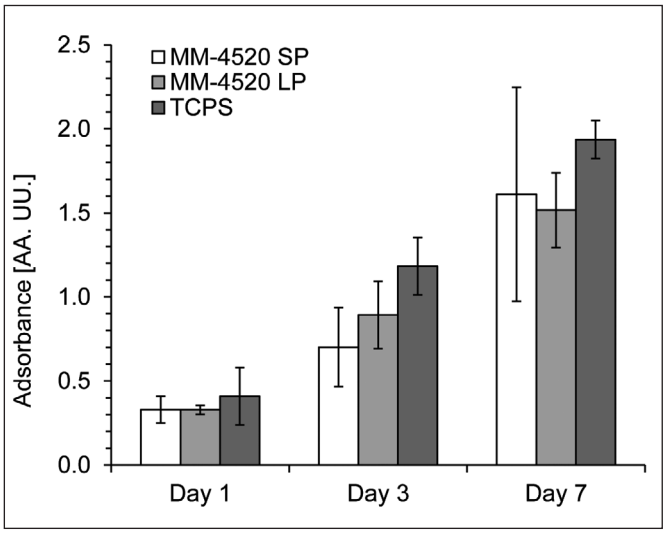

Fig. 4 - *Cell viability results obtained by MTT assay on MG63 cells seeded on MM-4520 scaffolds with small (SP, Ø < 150 µm) and large (LP, Ø = 150 ÷ 400 µm) pores. The control is represented by TCPS.*

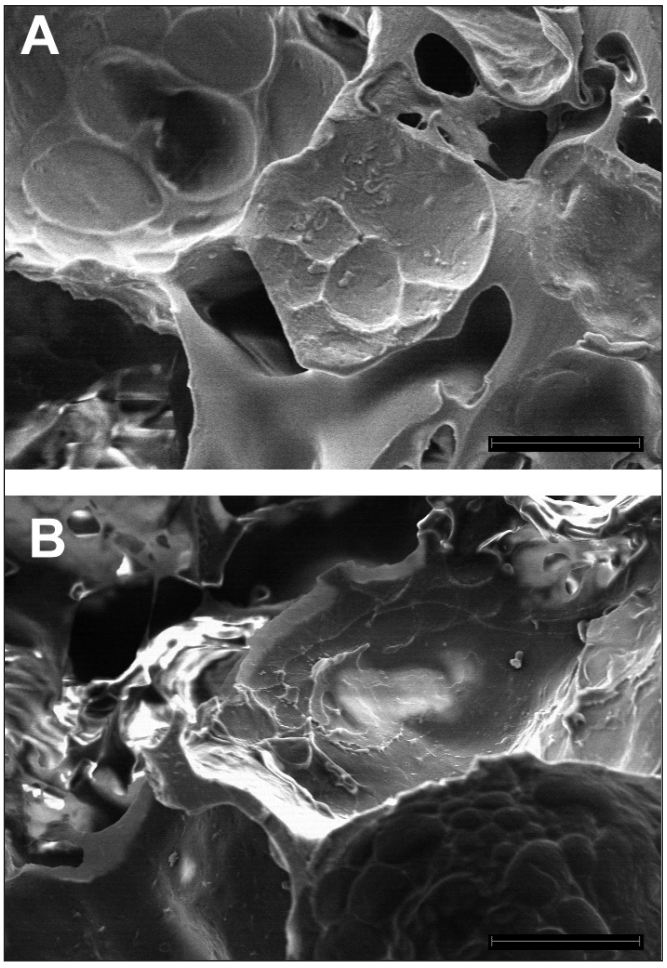

Fig. 5 - *MG63 cells morphology seven days after seeding onto the SP and LP scaffolds: (A) SP MM-4520 and (B) LP MM-4520 specimens. (Scale bar 50 µm.)*

Figure 5 reports SEM micrographs of the inner surfaces of both SP and LP structures, showing MG63 cells adhered and spread on their surface (after seven days of in vitro static culture). MG63 cells here were observed adhering and spreading onto the inner surface of the pores, regardless of the pore dimensions.

DISCUSSION

Shape Memory Polymer porous structures represent an interesting and promising platform for the design of new medical scaffolding technologies, especially in minimal invasive surgical procedures. SMPs are able to recover large deformations by using body temperature as a natural driving force triggering the Shape Memory Effect (SME). In this context, for instance, SMP stents have been studied (25), showing as a proof of concept the possibility to reduce catheter size for local mini-invasive delivery together with obtaining highly controlled and tailored deployment at body temperature.

SME has recently been regarded as a material property, just like density and specific heat, of all polymers (18). However, in order to exploit the thermo-responsive SME in medical applications in contact with the body, T_{trans} should be conveniently selected and/or tuned in a suitable specific range, compatible with the envisaged application. According to this specification, the thermal activated SME can enable driving the reshaping of device/product design and developing new fabrication techniques (18).

The study of new technologies to process advanced materials has been actively promoted (26,27), from fundamental to applied materials science, in different fields (28-31). Namely, the study on SMP foams has been originally proposed by Hayashi and Sokolowski (10, 32-34), and their applications in medical devices by the latter in cooperation with Prof. Yahia (8-10, 35). Moreover, it has been shown that polyurethane flexible foams with tunable shape fixability and cell size can be obtained without any major effects on shape recoverability (36). However, for such a class of SMP polyurethane-based foams, the foaming is in general obtained during polyurethane synthesis (i.e. gas foaming technique), reducing the possibility of tune shape, dimension, and porosity of the final structure.

We have shown, in a recent work (20), that a wide variety of properties can be obtained by coupling suitable manufacturing technologies and polymer classes without impairing their thermally activated SME. Solvent casting/particulate leaching methods, using gelatin particles with different sizes, has been exploited here and turned out to be a powerful tool for producing cellular materials with tunable porosity. Both qualitative assessment via SEM imaging and quantitative assessment via micro-CT indicated that SMP-based scaffolds with pore size, shape and interconnection have been easily obtained by selecting the shape and dimension of the starting porogen agent, according to the protocol developed by Draghi et al (23). This technique, moreover, represents an interesting tool because no major effects have been observed on transition temperature that triggers the SME: DMA analysis resulted in a slight variation of the T_{trans}, more likely because of the testing procedure, whereas the shape recovery showed a different recovery ability for the two porosities. Such a result needs to be further investigated in order to clarify whether it is a consequence of the preparation procedure or the specimen morphology (i.e. porosity).

A second important aspect that has been assessed in this study is a preliminary in vitro response of the scaffolds obtained with MG63 osteoblast-like cells. The biocompatibility is one of the main aspects to take into account when developing new materials for implantable devices (37). Some authors recently investigated this aspect on both compact and porous SMPs with different chemical composition. For instance, the biocompatibility of biodegradable SMP has been assessed using 3T3 cell line (38), their viability, proliferation, and metabolism resulting in similar results compared to tissue culture polystyrene. Rüder et al. (39) studied smooth muscle cells (SMC) and human umbilical vein endothelial cells (HUVEC) with electrospun scaffolds prepared from resorbable copolyetheresterurethane (PDC) in comparison to poly(vinylidene fluoride-co-hexafluoropropene) (PVDF) as reference material, which is established as a coating material of Drug Eluting Stent in clinical applications. Their results show that adhesion of human umbilical vein endothelial cells (HUVEC) were improved on PDC compared to PVDF, whereas almost no smooth muscle cells (SMC) attached to the scaffolds, indicating a cell-specific response of HUVEC towards the different fibrous structures.

A more specific previous study (40) on MM 5520 SMP, that belongs to the same family of SMP studied here, demonstrated that skin fibroblasts and gingival fibroblasts adhered and grew on the surface. Skin and gingival fibroblasts exhibited a flat, elongated cell morphology and a relatively smooth surface at 3 h of incubation. Furthermore, a confluent cell monolayer of both fibroblast cells was observed after 24 h and seven days onto the different materials. At higher magnification, typical surface features of fibroblasts were observed (40). Here, we observed and biochemically assessed the response to the scaffolds developed from MG63 osteo-blast like cells: MG63 cells were observed adhered and spreading onto the inner surface of the pores, regardless of the pore dimensions up to seven days of static culture.

This interesting result, similar to some others reported in the literature, indicates this class of materials to support the design of new biomedical devices, providing that materials and 3D structures are specifically tested in depth according to the envisaged applications.

CONCLUSIONS

In this work, the feasibility of Shape Memory Polymer three-dimensional structures via solvent casting/particulate leaching has been demonstrated. Scaffolds resulted in a tunable spectrum of size and dimension, preserving shape recovery ability. Moreover, MM-4520 SMP scaffolds were able to support in vitro cell adhesion and proliferation, without cytotoxic effect. This new class of SMP scaffolds could hence meet the needs of different medical applications and potentially be used in the design of new devices for mini-invasive surgical procedures.

Financial support: Luigi De Nardo acknowledges Ministero degli Affari Esteri Italia and Ministère des Affaires étrangères Québec for funding the project Materiali polimerici intelligenti per la realizzazione di dispositivi biomedici - Polymères intelligents pour diapositives biomédicaux in the context of Programma esecutivo Italia-Quebec. Luigi De Nardo also acknowledges Politecnico di Milano (Grant 5 per mille junior) and the Italian Ministry of Education, University and Research (MIUR-FIRB, Grant Number RBFR08XH0H).

Conflict of interest: The authors have no conflicts of interest to declare.

Address for correspondence:
Silvia Farè
Biomaterials Laboratory
Department of Bioengineering
Politecnico di Milano
P.zza Leonardo da Vinci, 32
20133 Milan - Italy
silvia.fare@polimi.it

REFERENCES

1. Fuchs KH. Minimally invasive surgery. Endoscopy 2002; 34: 154-9.
2. Li F, Zhang X, Hou J, et al. Studies on thermally stimulated shape memory effect of segmented polyurethanes. J Appl Polym Sci 1997; 64: 1511-6.
3. Lendlein A, Kelch S. Shape-memory polymers. Angew Chem Int Edit 2002; 41: 2034-57.
4. Lendlein A, Kratz K, Kelch S. Smart implant materials. Med Device technol 2005; 16: 12-4.
5. Gil FJ, Planell JA. Shape memory alloys for medical applications. P I Mech Eng H 1998; 212: 473-88.
6. Michiardi A, Aparicio C, Planell JA, Gil FJ. New oxidation treatment of NiTi shape memory alloys to obtain Ni-free surfaces and to improve biocompatibility. J Biomed Mater Res B 2006; 77: 249-56.
7. Yahia LH. Shape memory implants. Springer, Hong Kong, 2000.
8. De Nardo L, Alberti R, Cigada A, Yahia L, Tanzi MC, Fare S. Shape memory polymer foams for cerebral aneurysm reparation: Effects of plasma sterilization on physical properties and cytocompatibility. Acta Biomater 2009; 5: 1508-18.
9. Metcalfe A, Desfaits AC, Salazkin I, Yahia L, Sokolowski WM, Raymond J. Cold hibernated elastic memory foams for endovascular interventions. Biomaterials 2003; 24: 491-7.
10. Sokolowski W, Metcalfe A, Hayashi S, Yahia LH, Raymond J. Medical applications of shape memory polymers. Biomed Mater 2007; 2: S23-S27.
11. Lendlein A, Behl M, Hiebl B, Wischke C. Shape-memory polymers as a technology platform for biomedical applications. Expert Rev Med Devic 2010; 7: 357-79.
12. Mather PT, Luo X, Rousseau IA. Shape Memory Polymer Research. Ann Rev Mater Res 2009; 39: 445-71.
13. Ratna D, Karger-Kocsis J. Recent advances in shape memory polymers and composites: a review. J Mater Sci 2008; 43: 254-69.
14. Small W, Singhal P, Wilson TS, Maitland DJ. Biomedical applications of thermally activated shape memory polymers. J Mater Chem 2010; 20: 3356-66.
15. De Nardo L, Moscatelli M, Silvi F, Tanzi M, Yahia LH, Farè S. Chemico-physical modifications induced by plasma and ozone sterilizations on shape memory polyurethane foams. J Mater Sci Mater Med 2010; 21: 2067–78.
16. Tanzi MC, Bozzini S, Candiani G, et al. Trends in biomedical engineering: focus on Smart Bio-Materials and Drug Delivery. J Appl Biomater Biomech 2011; 9: 87-97.
17. Farè S, Valtulina V, Petrini P, et al. In vitro interaction of human fibroblasts and platelets with a shape-memory polyurethane. J Biomed Mater Res A 2005; 73: 1-11.
18. Huang W, Zhao Y, Wang C, et al. Thermo/chemo-responsive shape memory effect in polymers: a sketch of working mechanisms, fundamentals and optimization. J Polym Res 2012; 19: 1-34.
19. Lendlein A, Kelch S. Degradable, multifunctional polymeric biomaterials with shape-memory. Mater Sci Forum 2005; 492-493: 219-24.
20. De Nardo L, Bertoldi S, Tanzi MC, Haugen HJ, Faré S. Shape memory polymer cellular solid design for medical applications. Smart Mater Struct 2011; 20: 035004.
21. Witold S, Annick M, Shunichi H, L'Hocine Y, Jean R. Medical applications of shape memory polymers. Biomedical Materials 2007; 2: S23.
22. Zheng X, Zhou S, Li X, Weng J. Shape memory properties of poly(d,l-lactide)/hydroxyapatite composites. Biomaterials 2006; 27: 4288-95.
23. Draghi L, Resta S, Pirozzolo MG, Tanzi MC. Microspheres leaching for scaffold porosity control. J Mater Sci Mater Med 2005; 16: 1093-7.
24. Moore MJ, Jabbari E, Ritman EL, et al. Quantitative analysis of interconnectivity of porous biodegradable scaffolds with micro-computed tomography. J Biomed Mater Res A 2004; 71A: 258-67.
25. Yakacki CM, Shandas R, Lanning C, Rech B, Eckstein A, Gall K. Unconstrained recovery characterization of shape-memory polymer networks for cardiovascular applications.

Biomaterials 2007; 28: 2255-63.
26. Lattanzi L, Raney JR, De Nardo L, Misra A, Daraio C. Nonlinear viscoelasticity of freestanding and polymer-anchored vertically aligned carbon nanotube foams. J Appl Phys 2012; 111: 074314.
27. Misra A, Raney JR, De Nardo L, Craig AE, Daraio C. Synthesis and Characterization of Carbon Nanotube-Polymer Multilayer Structures. Acs Nano 2011; 5: 7713-21.
28. Ristori S, Ciani L, Candiani G, et al. Complexing a small interfering RNA with divalent cationic surfactants. Soft Matter 2012;8: 749-56.
29. Pezzoli D, Olimpieri F, Malloggi C, Bertini S, Volonterio A, Candiani G. Chitosan-Graft-Branched Polyethylenimine Copolymers: Influence of Degree of Grafting on Transfection Behavior. PLoS ONE 2012; 7: e34711.
30. Yang WS, Fuso L, Biamino S, et al. Fabrication of short carbon fibre reinforced SiC multilayer composites by tape casting. Ceram Int 2012; 38: 1011-8.
31. Pavese M, Fino P, Badini C, Ortona A, Marino G. HfB2/SiC as a protective coating for 2D Cf/SiC composites: Effect of high temperature oxidation on mechanical properties. Surf Coat Tech 2008; 202: 2059-67.
32. Tobushi H, Okumura K, Endo M, Hayashi S. Thermomechanical Properties of Polyurethane-Shape Memory Polymer Foam. J Intel Mat Syst Str 2001; 12: 283-7.
33. Sokolowski WM, Chmielewski AB, Hayashi S, Yamada T. Cold hibernated elastic memory (CHEM) self-deployable structures. Proceedings of SPIE - The International Society for Optical Engineering 1999; 3669: 179-85.
34. Hayashi S, Fujimura H. Shape Memory Polymer Foam. US Patent Specification 1991: 5,049,591.
35. De Nardo L, De Cicco S, Jovenitti M, Tanzi MC, Fare S. Shape memory polymer porous structures for mini-invasive surgical procedures. Proceedings of 8th Biennial ASME Conference on Engineering Systems Design and Analysis, ESDA2006, Torino, 2006.
36. Lee SH, Jang MK, Kim SH, Kim BK. Shape memory effects of molded flexible polyurethane foam. Smart Mater Struct 2007; 16: 2486-91.
37. Variola F, Vetrone F, Richert L, et al. Improving Biocompatibitity of Implantable Metals by Nanoscale Modification of Surfaces: An Overview of Strategies, Fabrication Methods, and Challenges. Small 2009; 5: 996-1006.
38. Xu SG, Zhang P, Zhu GM, Jiang YM. Effect of Biodegradable Shape-Memory Polymers on Proliferation of 3T3 Cells. J Mater Eng Perform 2011; 20: 807-11.
39. Rüder C, Sauter T, Becker T, et al. Viability, proliferation and adhesion of smooth muscle cells and human umbilical vein endothelial cells on electrospun polymer scaffolds. Clin Hemorheol Micro 2012; 50: 101-12.
40. Farè S, Valtulina V, Petrini P, et al. In vitro interaction of human fibroblasts and platelets with a shape-memory polyurethane. J Biomed Mater Res A 2005; 73A: 1-11.